

Structural transition and anisotropic properties of single-crystalline SrFe₂As₂

J.-Q. Yan,¹ A. Kreyssig,^{1,2} S. Nandi,^{1,2} N. Ni,^{1,2} S. L. Bud'ko,^{1,2} A. Kracher,¹ R. J. McQueeney,^{1,2} R. W. McCallum,^{1,3}
T. A. Lograsso,¹ A. I. Goldman,^{1,2} and P. C. Canfield^{1,2}

¹Ames Laboratory, US DOE, Iowa State University, Ames, Iowa 50011, USA

²Department of Physics and Astronomy, Iowa State University, Ames, Iowa 50011, USA

³Materials Science and Engineering, Iowa State University, Ames, Iowa 50011, USA

(Received 18 June 2008; published 23 July 2008)

Platelike single crystals of SrFe₂As₂ as large as 3 × 3 × 0.5 mm³ have been grown out of Sn flux. The SrFe₂As₂ single crystals show a structural phase transition from a high-temperature tetragonal phase to a low-temperature orthorhombic phase at $T_o=198$ K, and do not show any sign of superconductivity down to 1.8 K. The structural transition is accompanied by an anomaly in the electrical resistivity, Hall resistivity, specific heat, and the anisotropic magnetic susceptibility. In an intermediate temperature range from 198 to 160 K, single-crystal x-ray diffraction suggests a coexistence of the high-temperature tetragonal and the low-temperature orthorhombic phases.

DOI: 10.1103/PhysRevB.78.024516

PACS number(s): 74.70.Dd, 61.50.Ks, 65.40.Ba, 72.15.-v

The recent discovery of high transition temperature (T_c) superconductivity in fluorine-doped RFeAsO (R = rare earth) and K-doped AFe₂As₂ (A = Sr and Ba) has attracted extensive attention in scientific community.^{1,2} RFeAsO with the ZrCuSiAs-type structure and AFe₂As₂ with the ThCr₂Si₂-type structure share the same structural unit of (Fe₂As₂) layers. The (Fe₂As₂) layers are separated by (R_2O_2) layers in RFeAsO and by simple A layers in AFe₂As₂. Partial substitution of A^{2+} by K^+ or Cs^+ induces superconductivity with T_c up to 38 K.²⁻⁴ Studies of polycrystalline samples have revealed phase transitions at $T_o=140$ and 205 K for BaFe₂As₂ and SrFe₂As₂, respectively.^{5,6} At $T_o=140$ K for BaFe₂As₂, the structural transition from a high-temperature tetragonal phase to a low-temperature orthorhombic phase is thought to be accompanied by a magnetic phase transition.⁵ However, whether a similar structural transition takes place in SrFe₂As₂ at $T_o=205$ K concomitantly with the magnetic anomaly is still an open question. Indeed, C. Krellner *et al.*⁶ suggests the occurrence of a similar combination of a structural and a magnetic transition based on unpublished results measured on polycrystalline samples. This question is of great importance due to the fact that a similar combination of structural and magnetic phase transitions was observed in RFeAsO.⁷

High quality, sizable single crystals are necessary in order to study the anisotropic properties of the compounds and details of the crystallographic structure. Ni *et al.*⁸ successfully grew BaFe₂As₂ single crystals out of Sn flux and studied the crystallographic, anisotropic magnetic, and transport properties. However, ~1% Sn was incorporated into the BaFe₂As₂ lattice and modifies the physical properties relative to those of polycrystalline samples. Whether SrFe₂As₂ lattice is susceptible to Sn incorporation remains to be clarified. Here, we report the growth of SrFe₂As₂ single crystals out of Sn flux and subsequent measurements of the anisotropic physical properties, including x-ray diffraction studies of the structural transition.

Single crystals of SrFe₂As₂ were grown out of Sn flux. Elemental Sr, Fe, and As were fired at 850 °C for 12 h and 900 °C for 20 h with intermediate grinding. The prefired pellet, which contains mainly SrFe₂As₂ with ~5% FeAs im-

purity, was broken into smaller pieces and added to Sn flux in the ratio of [SrFe₂As₂]:Sn = 1:48 and placed in a 2 ml crucible. A catch crucible containing quartz wool was mounted on top of growth crucible and both were sealed in a silica ampoule under approximately 1/3 atmosphere of argon gas. The packing and assembly of the growth ampoule were performed in air since the prefired pellet is stable in air. The sealed ampoule was heated to 1000 °C and cooled over 36 h to 500 °C in a programmable furnace. At 500 °C, the Sn was decanted from the SrFe₂As₂ crystals. We note that some pieces of the prefired pellets are still undissolved in the growth crucible. Raising the ratio of [SrFe₂As₂]:Sn leads to more residual undissolved SrFe₂As₂.

As-grown crystals are platelike with a typical dimension of 1–2 × 1–2 × 0.1–0.5 mm³. Some crystals manifest linear dimensions as large as 3–4 mm as shown in the inset of Fig. 1. Room-temperature powder x-ray diffraction confirmed that the crystals are single phase with lattice parameters of $a=3.926(3)$ Å and $c=12.42(1)$ Å, consistent with previous reports.^{4,6} Wavelength-dispersive x-ray analysis (WDS) was performed on a JEOL JXA-8200 electron microprobe at 15 kV acceleration voltage and ~10 nA beam current. Elemental analysis confirmed the atomic ratio of 1:2:2 and observed about 0.3% (atomic) Sn in the bulk, a factor of 3 times less Sn than the BaFe₂As₂ crystals grown in a similar manner.⁸

Single-crystal x-ray diffraction measurements were performed on a standard four-circle diffractometer using Cu K_α radiation from a rotating anode x-ray source, selected by a Ge(1 1 1) monochromator. For these measurements, a platelike single crystal with dimensions of 3 × 2 × 0.5 mm³ was selected. The sample was mounted on a flat copper sample holder in a closed cycle displacer cryogenic refrigerator with the (001)–(110) reciprocal-lattice plane coincident with the scattering plane. The diffraction patterns were recorded for temperatures between 10 and 300 K. The mosaicity of this crystal was 0.035° full width at half maxima for the (0 0 10) reflection, indicating the excellent quality of the single crystal.

Magnetic properties were measured with a quantum design (QD) magnetic property measurement system (MPMS).

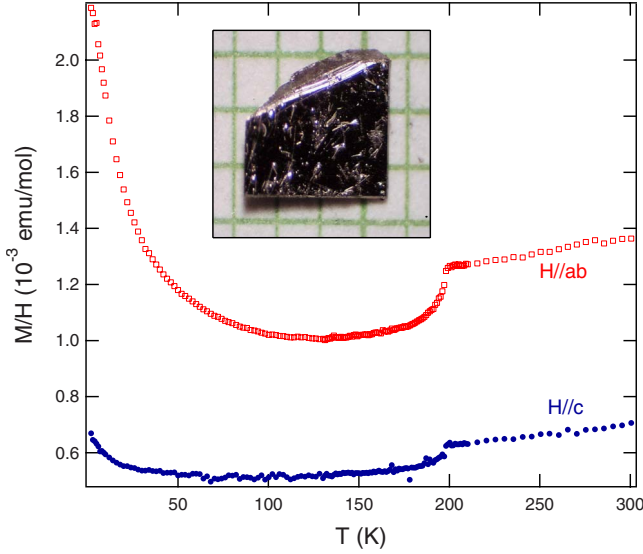


FIG. 1. (Color online) Temperature dependent, anisotropic magnetization measured at a magnetic field of 50 kOe for SrFe_2As_2 . The inset shows the photograph of a single crystal on a mm grid. The crystallographic c axis is perpendicular to the plane of the plate. A few droplets of Sn flux can be seen on the surface.

The temperature dependent specific heat as well as magnetic-field and temperature dependent electrical transport data were collected using a QD physical property measurement system (PPMS). Electrical contact was made to the samples using Epotek H20E silver epoxy to attach Pt wires in a four-probe configuration. Hall measurements were performed in a QD PPMS instrument using the four probe ac ($f=16$ Hz, $I=1$ mA) technique with the current flowing in the ab plane approximately parallel to the a axis and the field parallel to the c axis. To eliminate the effect of a misalignment of the voltage contacts, the Hall measurements were taken for two opposite directions of the applied field, H and $-H$, and the odd component, $[\rho_H(H) - \rho_H(-H)]/2$, was taken as the Hall resistivity.

As shown in Fig. 1, magnetic measurements clearly show the anisotropy in the magnetic susceptibility $\chi = M(T)/H$ and a transition at $T_o = 198$ K. The transition temperature is slightly lower than that observed for polycrystalline samples.⁶ Compared with the temperature dependence for polycrystalline samples, three prominent features are noteworthy: (1) Over the whole temperature range, there is a clear anisotropy with $\chi_{ab} > \chi_c$. (2) Below room temperature, both χ_{ab} and χ_c decrease linearly as the sample is cooled with a small slope until T_o . At T_o , they show a step-like change. Below T_o , both curves show a minimum in the temperature interval $100 \text{ K} < T < 150 \text{ K}$. This temperature dependence is different from that of polycrystalline samples reported by Krellner *et al.*,⁶ but agrees with that by Pfisterer and Nagorsen.⁹ (3) Below ~ 100 K the susceptibility becomes even more anisotropic, with a clear Curie-Weiss-like tail for $H \parallel ab$. The effective moment associated with this tail is $0.35 \mu_B/\text{f.u.}$ The fact that this tail is so anisotropic argues that it is not associated with polycrystalline impurities within the residual Sn flux on the surface, but rather associated with the bulk, crystalline sample.

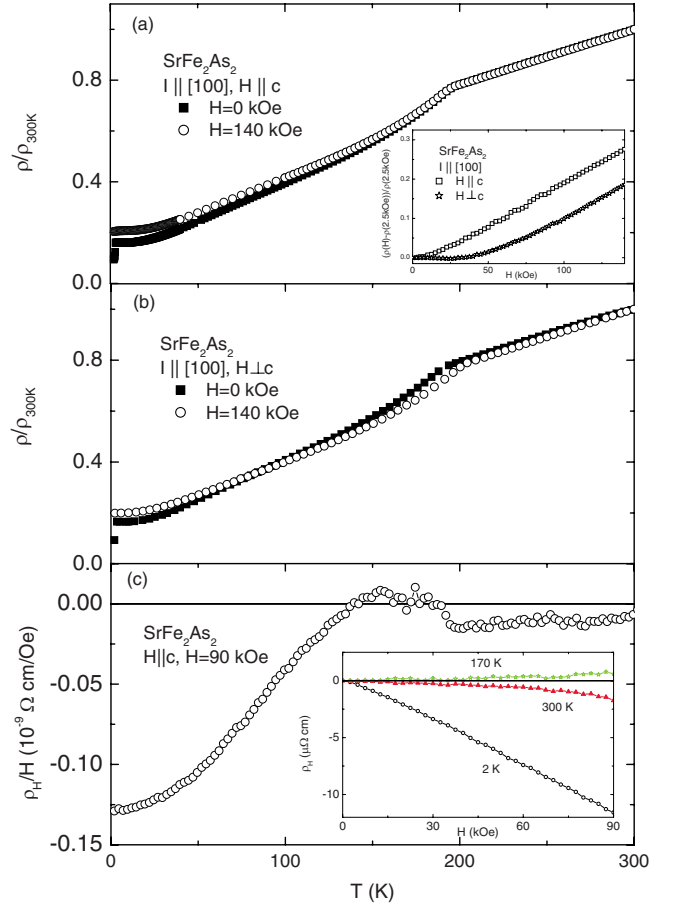


FIG. 2. (Color online) [(a) and (b)] Temperature dependence of normalized in-plane electrical resistivity in zero field and in an applied magnetic field of 140 kOe. The inset shows the field dependence of the magnetoresistivity $\Delta\rho/\rho_0$ measured at 2 K with magnetic field applied parallel and perpendicular to the c axis. Note small features in the $H=0$ data at low temperatures are due to small amounts of Sn (flux) on the sample. (c) Temperature dependence of the Hall resistivity divided by applied magnetic field. Inset shows a close to linear magnetic-field dependence of the Hall resistivity at three salient temperatures: 300, 170, and 2 K.

Figure 2(a) presents the temperature dependence of the in-plane electrical resistivity $\rho(T)$. $\rho(T)$ decreases with cooling and shows a sudden drop at $T_o = 198$ K. The residual resistivity ratio (RRR) of $\rho_{300 \text{ K}}/\rho_{2 \text{ K}} \sim 6$ is smaller than the value of 32 of polycrystalline samples⁶ and larger than ~ 3 of similar single crystals grown out of Sn flux.¹⁰ The application of a magnetic field of 140 kOe parallel to the c axis has no effect on the phase transition at $T_o \sim 198$ K but slightly enhances the resistivity below ~ 150 K. On the other hand, the application of a 140 kOe field perpendicular to the c axis shifts the transition upward by as much as ~ 10 K.

The inset of Fig. 2(a) shows the field dependence of the magnetoresistivity (MR) measured at 2 K. When the magnetic field is applied along the c axis, the MR increases with field and reaches $\sim 27\%$ by 140 kOe. In contrast, the MR starts to increase only for $H > 30$ kOe and only reaches $\sim 18\%$ by 140 kOe when the magnetic field is applied in the ab plane. The observed value is consistent with the experimental results in Ref. 10 for field applied in the ab plane.

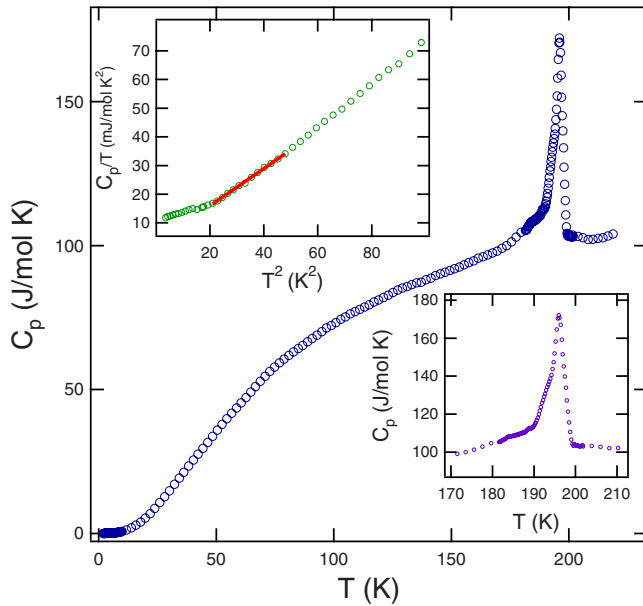


FIG. 3. (Color online) Temperature dependent specific heat of SrFe_2As_2 . Upper inset: C_p/T as a function of T^2 for low-temperature data. Lower inset: expanded view near the $T_0=198$ K phase transition.

The Hall resistivity [Fig. 2(c)] is almost temperature independent at high temperatures, but has a sharp break just below 200 K, consistent with a structural phase transition. On further cooling, initially the Hall resistivity increases slightly, and then, below ~ 150 K monotonically decreases, reaching, at 2 K, a value close to that observed for BaFe_2As_2 .⁸

The temperature dependent specific-heat data are presented in Fig. 3. A sharp feature at $T=198$ K (lower inset) indicates the transition temperature which is consistent with that determined from magnetic and transport measurements. The upper inset to Fig. 3 shows the low-temperature C_p/T data plotted as a function of T^2 . The data follow the standard power law, $C_p = \gamma T + \beta T^3$. Below $T^2 \sim 20$ K² the data deviate from linearity possibly associated with residual Sn flux. The Debye temperature Θ_D could be estimated from $\beta = 12\pi^4 n k_B / (5\Theta_D^3)$, where $n=5$ is the number of atoms per formula unit for SrFe_2As_2 . The fitting for $20 < T^2 < 45$ K² yields $\gamma = 33$ mJ/mol K² and $\beta = 0.64$ mJ/mol K⁴ ($\Theta_D = 248$ K) similar to those of BaFe_2As_2 .⁸

The transition temperature determined from the magnetization, electrical resistivity, Hall resistivity, and specific-heat measurements agrees with each other. The SrFe_2As_2 single crystals have comparable lattice parameters and similar transition temperatures as the polycrystalline material.⁶ This is consistent with the WDS analysis which indicates significantly less Sn is incorporated into the single crystalline SrFe_2As_2 material in comparison to the reported BaFe_2As_2 crystals.⁸ To determine whether there is a structural transition at T_0 as observed in the isostructural BaFe_2As_2 ,^{5,8} we performed a single-crystal x-ray diffraction study. As illustrated in Fig. 4, below 160 K, the splitting of the (1 1 10) reflection was observed in $(\xi\xi 0)$ scans, whereas the shape of the (0 0 10) reflection is unchanged in both $(\xi\xi 0)$ and (00ξ) scans. This behavior is consistent with a tetragonal-to-orthorhombic

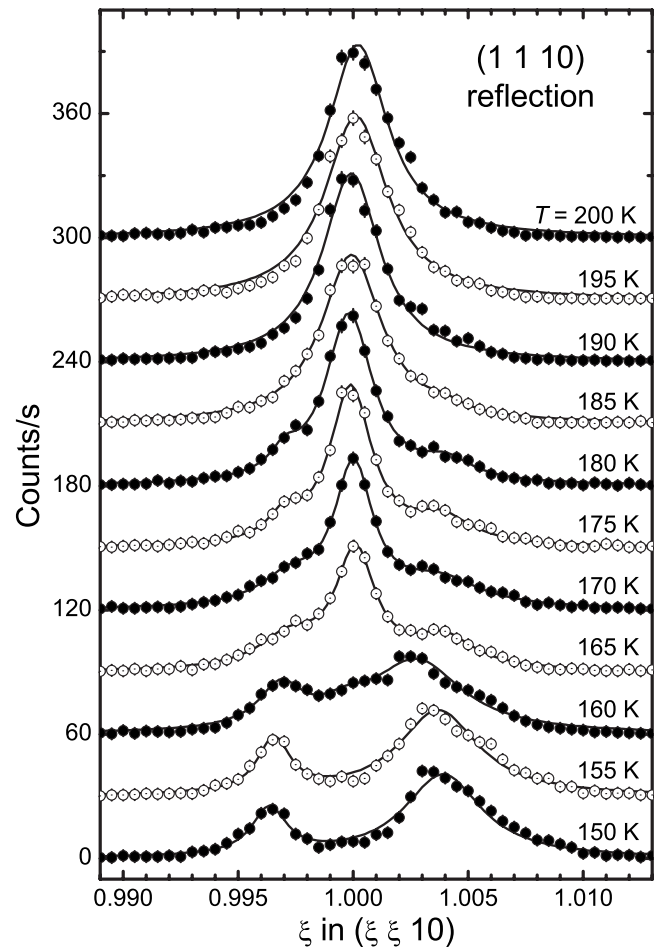


FIG. 4. X-ray diffraction scans along the (110) direction through the position of the tetragonal (1110) reflection for selected temperatures. The lines represent the fitted curves to obtain the reflection positions for the data shown in Fig. 5. The offset between every data set is 30 counts/s.

phase transition with a distortion along the diagonal (110) direction and a transition from the space group $I4/mmm$ to $Fmmm$, similar to that observed in the BaFe_2As_2 compound.⁸ In an intermediate temperature range between 190 and 160 K, reflections related to the orthorhombic phase appear to coexist with reflections related to the tetragonal phase as shown in the $(\xi\xi 0)$ scans in Fig. 4. However, no significant difference was observed between measurements with decreasing and increasing temperatures as might be expected from a hysteretic first-order transition as reported in Ref. 6. We note that the split reflections are not equal in intensity or width at low temperatures, perhaps indicating an unequal “twin domain” population. However, we also note that a crystallographic structure with symmetry lower than the orthorhombic can yield a similar diffraction pattern at low temperature and cannot be excluded by the present study.

The lattice parameters have been determined by measurements of selected scans for the (0 0 10) and (1 1 10) reflections. By analyzing the position of the (0 0 10) reflection in longitudinal (00ξ) scans, the c -lattice parameter can be determined. The in-plane a and b -lattice parameters have been calculated based on the distance between the reflections close

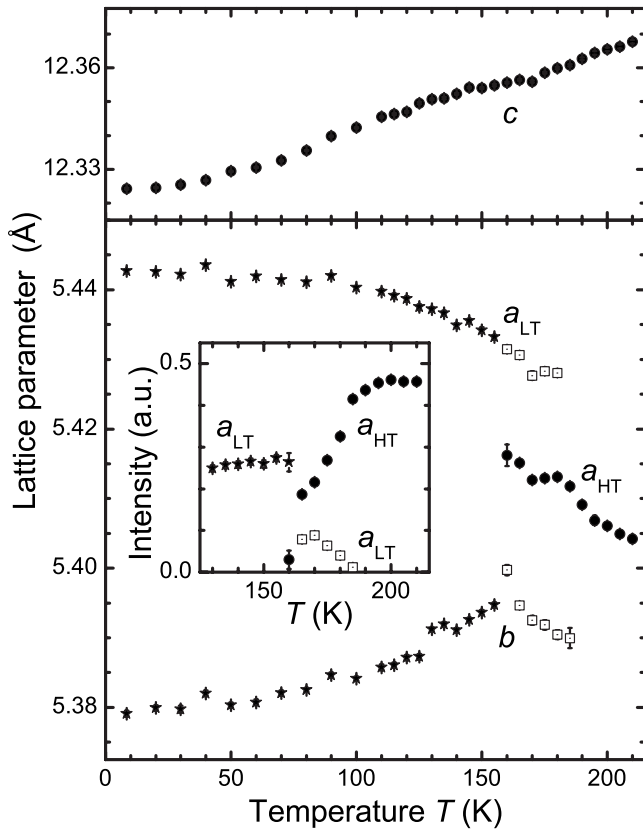


FIG. 5. Lattice parameters for the tetragonal and orthorhombic phases as extracted from the data shown in Fig. 4 for the (1110) reflection and the (0010) reflection (not shown). To allow direct comparison of both phases, the lattice parameter a of the tetragonal phase is given as $a_{HT} = \sqrt{2}a$. The inset shows the intensity of the reflections related to the lattice parameter a in both phases. The error bars represent the relative precision, the absolute error is method related and significantly larger.

to the tetragonal (1 1 10) position and the (0 0 10) reflection in transverse scans along the $(\xi\xi0)$ direction. The results are shown in Fig. 5 together with an analysis of the intensity of

the characteristic reflections. Between 10 and 160 K, the difference in the orthorhombic a - and b -lattice parameters decreases monotonically with increasing temperature. Surprisingly, the difference between the in-plane lattice parameters stays nearly constant between 160 K and the transition to the tetragonal phase above 190 K. In the same intermediate temperature range, however, the sign of the thermal-expansion coefficient for the orthorhombic b direction changes, coincident with the abrupt appearance of the central reflection related to the tetragonal phase at 160 K (see inset in Fig. 5). These observations suggest a more complex nature for this phase transition even though the transition from the space group $I4/mmm$ to $Fmmm$ can be second order. We also note that while the structure in this intermediate temperature range can be described in terms of a coexistence between the high-temperature tetragonal phase and the low-temperature orthorhombic phase, a complex superstructure of the high-temperature phase with an additional order parameter could likewise yield the observed set of three reflections. It should be noted that measurements of $M(T)/H$ on the crystal used for Figs. 4 and 5 showed only one transition at $T_o = 198$ K.

In conclusion, we have successfully grown sizable single crystals of SrFe_2As_2 out of Sn flux and studied anisotropic thermodynamic and transport properties as well as the structural transition. Electrical resistivity, Hall resistivity, specific heat, and the anisotropic magnetic susceptibility demonstrate a transition at $T_o = 198$ K. The magnetic susceptibility, $\chi = M/H$, is anisotropic, with $\chi_{ab} > \chi_c$ for $2 \text{ K} < T < 300 \text{ K}$. While the transition appears to be insensitive to $H \parallel c = 140 \text{ kOe}$, it does shift upward by $\sim 10 \text{ K}$ for $H \parallel ab = 140 \text{ kOe}$. As evidenced by the single-crystal x-ray diffraction study, a similar structural phase transition as in BaFe_2As_2 from a high-temperature tetragonal phase to a low-temperature orthorhombic phase takes place at $T_o = 198 \text{ K}$.

Work at the Ames Laboratory was supported by the U.S. Department of Energy—Basic Energy Sciences under Contract No. DE-AC02-07CH11358. The authors would like to acknowledge useful discussions with E. D. Mun, M. Tillman, M. G. Kim, and G. E. Rustan.

¹Y. Kamihara, T. Watanabe, M. Hirano, and H. Hosono, *J. Am. Chem. Soc.* **130**, 3296 (2008).

²M. Rotter, M. Tegel, and D. Johrendt, arXiv:0805.4630 (unpublished).

³G. F. Chen, Z. Li, G. Li, W. Z. Hu, J. Dong, X. D. Zhang, P. Zheng, N. L. Wang, and J. L. Luo, arXiv:0806.1209 (unpublished).

⁴K. Sasmal, B. Lv, B. Lorenz, A. M. Guloy, F. Chen, Y.-Y. Xue, and C.-W. Chu, arXiv:0806.1301 (unpublished).

⁵M. Rotter, M. Tegel, D. Johrendt, I. Schellenberg, W. Hermes, and R. Pöttgen, *Phys. Rev. B* **78**, 020503(R) (2008).

⁶C. Krellner, N. Caroca-Canales, A. Jesche, H. Rosner, A. Or-

meci, and C. Geibel, arXiv:0806.1043 (unpublished).

⁷See, for example, C. de la Cruz, Q. Huang, J. W. Lynn, J. Li, W. Ratcliff II, J. L. Zarestky, H. A. Mook, G. F. Chen, J. L. Luo, N. L. Wang, and P. Dai, *Nature (London)* **453**, 899 (2008).

⁸N. Ni, S. L. Bud'ko, A. Kreyssig, S. Nandi, G. E. Rustan, A. I. Goldman, S. Gupta, J. D. Corbett, A. Kracher, and P. C. Canfield, *Phys. Rev. B* **78**, 014507 (2008).

⁹M. Pfisterer and G. Nagorsen, *Z. Naturforsch. B* **38**, 811 (1983).

¹⁰G. F. Chen, Z. Li, J. Dong, G. Li, W. Z. Hu, X. D. Zhang, X. H. Song, P. Zheng, N. L. Wang, and J. L. Luo, arXiv:0806.2648 (unpublished).